CrystEngComm

Revisiting the structural homogeneity of NU-1000, a Zr-based Metal-Organic Framework

Journal:	*CrystEngComm*
Manuscript ID	CE-COM-03-2018-000455.R1
Article Type:	Communication
Date Submitted by the Author:	02-May-2018

Complete List of Authors:	Islamoglu, Timur; Northwestern University, Department of Chemistry Otake, Ken-ichi; Northwestern university Li, Peng; Northwestern University, Department of Chemistry Buru, Cassandra; Northwestern University, Chemistry Peters, Aaron; Northwestern Universtiy, Department of Chemistry Akpinar, Isil; University College London, Chemical Engineering Garibay, Sergio; Northwestern university Farha, Omar; Northwestern University, Department of Chemistry

CrystEngComm

COMMUNICATION

Revisiting the structural homogeneity of NU-1000, a Zr-based Metal-Organic Framework

Received 00th January 20xx,
Accepted 00th January 20xx

DOI: 10.1039/x0xx00000x

www.rsc.org/

Timur Islamoglu,*[a] Ken-ichi Otake,[a] Peng Li,[a] Cassandra T. Buru,[a] Aaron W. Peters,[a] Isil Akpinar,[a] Sergio J. Garibay[a] and Omar K. Farha*[a,b]

Synthesis and activation of phase-pure and defect-free metal–organic frameworks (MOFs) are essential for establishing accurate structure-property relationships. Primarily suffering from missing linker and/or node defects, Zr_6-based MOFs can have polymorphs, structures with the identical linker and node but different connectivity, which can create multiple phases in a sample thatcomplicates the characterization. Here, we report the synthesis of phase-pure NU-1000, a mesoporous Zr_6-based MOF that typically contains a significant secondary phase within the individual crystallites. Large biomolecules and smaller inorganic molecules have been installed in NU-1000 as probes to verify the near elimination of the microporous secondary-phase. Obtaining structurally homogenous MOFs will assist the design of new materials with distinct structural features.

Introduction

In the last two decades, an ever growing interest in metal–organic frameworks (MOFs), crystalline materials capable of achieving permanent porosity composed of metal ions/clusters spaced with organic linkers, has led to the realization of thousands of MOFs with unique properties.[1] Among the reported MOFs, hexanuclear zirconium-based MOFs possess high chemical and thermal stability, making them extremely popular candidates for multiple applications ranging from gas storage to catalysis.[2-3] Since the discovery of the first Zr_6 cluster based-MOF, UiO-66,[4] many Zr_6-based MOFs with larger pore dimensions and geometries have been designed.[2, 5-6] Reticular chemistry[7] allows control over the connectivity (i.e. the number of ligands coordinated to each Zr_6 cluster) of the inorganic nodes ranging from 12-, 10-, 8-, or 6-connected, resulting in a variety of topologies including, but not limited to **csq**,[8-9] **scu**,[10-12] **ftw**,[13-15] **spn**,[16] **reo**[17] and **fcu**.[4] While structural irregularities or defects in these MOFs often indicate missing linkers and/or nodes, inhomogeneity is also possible if multiple phases can be constructed from identical secondary building units (SBUs, i.e. ligands and metal clusters).[18-20] These phases are called polymorphs, and the resulting MOFs differ in crystal packing arrangements and/or conformations.[2, 17] For example, the combination of a tetratopic porphyrin linker and a Zr_6 cluster gives rise to at least six unique MOFs.[12, 15, 21-23] The different connectivity of the various topologies manifests in distinctive physical (i.e. pore/aperture size/shape, morphology of crystal) and chemical (i.e. different number of reactive –OH sites) properties. Having multiple topologies in one sample significantly complicates the characterization and computational modelling of a material, where only phase-pure structures typically are considered. Therefore, to establish strong structure-property relationships, the studied MOFs should be close to phase-pure. Although using an excess amount of a monodentate modulator during the synthesis often suffices for isolating many phase-pure Zr-MOFs,[24-27] some systems require more effort to avoid polymorphs.

NU-1000, a Zr_6-based MOF composed of $Zr_6(\mu_3\text{-}OH)_4(\mu_3\text{-}O)_4(OH)_4(OH_2)_4$ nodes and tetratopic pyrene-based linkers [$TBAPy^{4-}$, 1,3,6,8-tetrakis(*p*-benzoate)pyrene] with **csq** topology, possesses mesoporous 31 Å hexagonal channels and microporous 12 Å triangular channels with orthogonal 10 x 8 Å windows connecting the channels (Figure 1).[8, 28] Due to its high surface area, chemical and thermal stability, hierarchical pore structure and relative ease of scalability, NU-1000 has been heavily investigated for several potential applications such as catalysis and support materials on which to install additional functionality.[29-38] Phase purity in NU-1000 pertains not to the bulk samples, but also to individual crystallites. In a typical synthesis of NU-1000 with benzoic acid as a modulator, NU-901 structural motifs are present in the middle of the crystallites.[8] NU-901 is a polymorph which crystallizes in the **scu** net, and has higher density compared to the **csq** net NU-1000 (0.704 vs 0.486 g cm^{-3}).[39] Single crystal X-ray diffraction (XRD) analysis revealed extra electron density with approximately 25% occupancy located in the center of the mesoporous channels of NU-1000.[8] Coupled with computational models, this density is attributed to the NU-901 phase. Note, care must be taken to not eliminate the possibility of secondary phases in single crystal X-ray diffraction data by assuming the presence of solvent and using SQUEEZE to remove this electron density. Further

a. Department of Chemistry, Northwestern University, 2145 Sheridan Road, Evanston, Illinois 60208, United States
b. Department of Chemistry,Faculty of Science King Abdulaziz University Jeddah 21589, Saudi Arabia
*Corresponding authors:timur.islamoglu@northwestern.edu
o-farha@northwestern.edu
Electronic Supplementary Information (ESI) available: [details of any supplementary information available should be included here]. See DOI: 10.1039/x0xx00000x

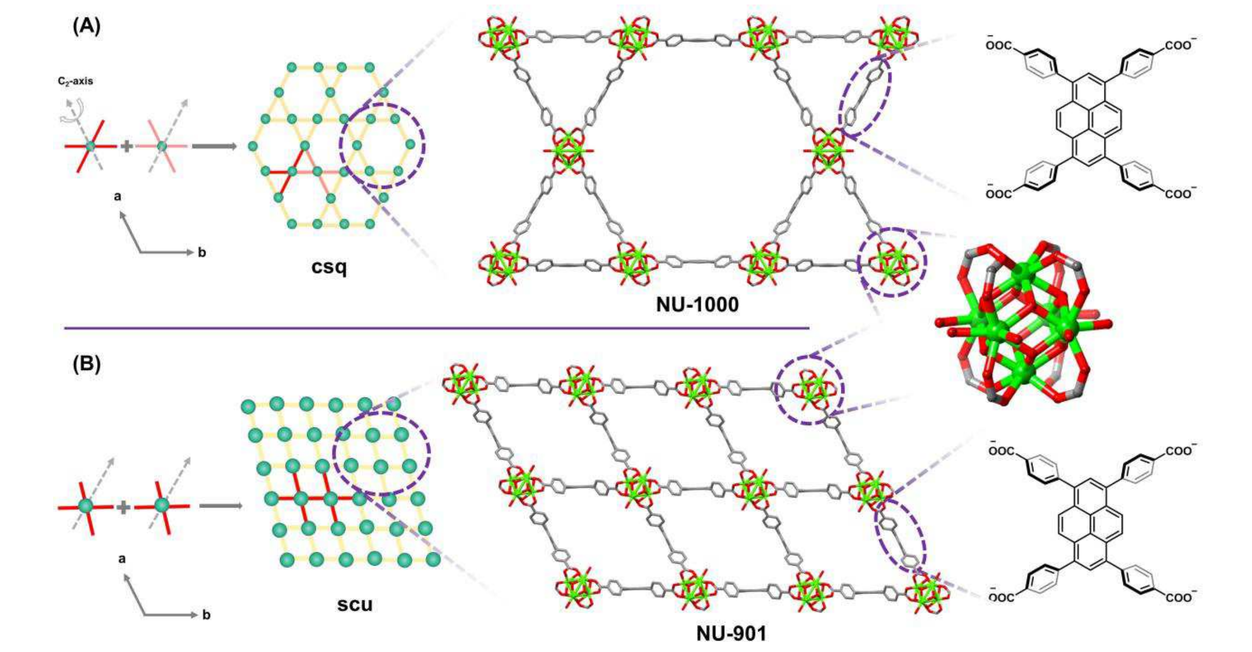

Figure 1. (A) Schematic representations of the alternating Zr_6 node resulting in csq topology NU-1000. (B) Schematic representations of the parallel Zr_6 node resulting in scu topology NU-901.

evidence of this secondary phase can be seen in scanning electron microscopy (SEM) images (Figure 2A), where the center of the hexagonal rod-shaped crystal appears "rough". Interestingly, the rest of the crystals shows six smooth rectangular facets forming the hexagonal rods, implying that secondary phase primarily exists in the center of the crystal where seeding is thought to occur. Several other experiments also confirm the presence of a microporous regime in the center of the crystallites.[40-41]

Both NU-1000 and NU-901 are 8-connected, so the polymorphism arises from the relative alignment of the C_2 axes along the nodes (Figure 1). Nodes in the MOF with **csq** topology, NU-1000, are angled 120° to each other whereas in NU-901 with **scu** topology they are parallel. The alignment of the nodes is dictated by the conformation of adjacent benzoate groups on the $TBAPy^{4-}$ linkers (Figure 1). Truhlar and coworkers recently calculated that introducing bulky groups (i.e CF_3 or *tert*-butyl) to the $TBAPy^{4-}$ at the 2- and 7-carbon positions (the carbon atom between two benzoate groups) stabilizes the rotamer present in NU-1000 and precludes the formation of NU-901 phase.[42] While this method could result in phase-pure **csq** net topology, the linker synthesis would be much more challenging than $TBAPy^{4-}$ synthesis. As an alternative, Penn and coworkers employed biphenyl-4-carboxylic acid as the modulator instead of benzoic acid to induce a larger steric effect around the node that prevented the formation of microporous NU-901.[39] However, the lengthy modulator can be problematic when applying this method to other systems with channels larger than that of NU-1000. For example, the isoreticular expansion of NU-1000 to NU-1003 enlarges the hexagonal channels to 44 Å and accommodates larger biomolecules.[43] Since the mesoporous channels are larger, NU-1003 would require a modulator lengthier than biphenyl-4-carboxylic, thereby limiting practical use for large-scale synthesis due to synthetic complexity and reduced solubility of longer aromatic chain length ligands. Therefore, simpler methods for obtaining phase-pure NU-1000 are still needed.

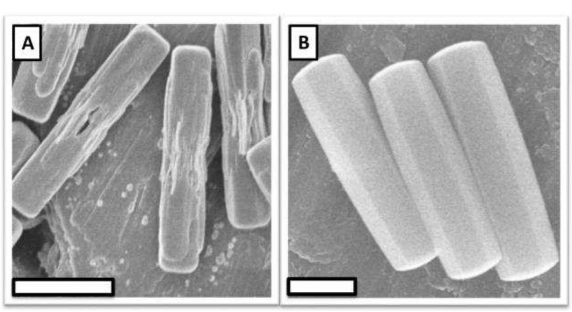

Figure 2. SEM images of NU-1000 (A) and NU-1000-TFA (B) crystals. Scale bars are 2 microns.

Here, we report the use of trifluoroacetic acid (TFA) as a co-modulator, along with benzoic acid, in the synthesis of NU-1000 to help eliminate the NU-901 phase formation during the early stage of crystallization of NU-1000. While the role of the TFA is still under investigation, the presence of TFA can inhibit the rate of H_4TBAPy linker deprotonation since TFA is much stronger acid (pK_a=0.3) than benzoic acid (pK_a=4.2). This suggests that the vast majority of the TFA will be ionized while the majority of benzoic acid will be non-ionized at the reaction conditions (pH= ~1.35). Additionally, Lewis acidity of the Zr_6 node would be increased when TFA is coordinated to the node instead of benzoic acid, which translates into stronger ionic Zr–carboxylate

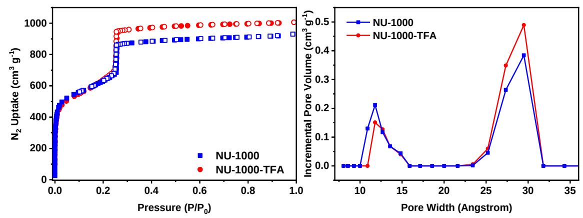

Figure 3. (A) Nitrogen isotherms of NU-1000 and NU-1000-TFA, (B) corresponding pore size distribution.

bond.[44] The resulting alteration of the coordination equilibrium during the crystal growth process yields nearly phase-pure NU-1000 crystals.

Results and discussion

SEM images of NU-1000 crystals synthesized using previously reported method yields crystals with "rough" surfaces in the center while MOF crystals synthesized using TFA as co-modulator (referred as NU-1000-TFA) display hexagonal rods with six undisturbed rectangular facets throughout the crystals (Figure 2), suggesting the absence of the NU-901 phase. While the crystal morphology of MOFs can yield information regarding the inner-structure of the material, further evidence is required to confirm a MOF's phase-purity. The N_2 isotherm of NU-1000-TFA exhibits a larger mesoporous step, which translates to larger total pore volume compared to NU-1000 (Figure 3, Table 1). Brunauer-Emmett-Teller (BET) theory calculations reveal that NU-1000-TFA, NU-1000, and NU-901 have similar surface areas (Table 1). Since NU-901 is a microporous MOF with a similar BET surface area compared to NU-1000, the elimination of NU-901 phase should have a pronounced effect on total pore volume but not on the specific surface area. Additionally, the percent of micropore volume in the samples was reduced from 43 to 34% in NU-1000 to NU-1000-TFA (Table 1), which is consistent with the elimination of the NU-901 phase.

Table 1. Surface area, micropore and total pore volume of MOFs.

MOF	BET Surface area (m^2/g)	Micro/total pore volume (cc/g)	Micropore volume (%)
NU-1000	2220	0.544/1.259	43
NU-1000-TFA	2180	0.466/1.369	34
NU-901	2100	0.677/0.780	87[a]

[a]Less than 100% micropore volume in NU-901 can be attributed to the defects in the crystal.[45]

Despite the utility of powder X-ray diffraction (PXRD) patterns in determining phase-purity of solids, the diffraction analysis of NU-1000-TFA was complicated because of similar unit cells of NU-1000 and NU-901, creating overlap of the main diagnostic peaks for these MOFs. Instead, we employed probe molecules to determine if the microporous NU-901 had been eliminated. First, dye (AlexaFluor-647) labeled insulin (insulin647) was installed in NU-1000 and NU-1000-TFA by soaking the MOFs in a protein solution for 1 day. Because of its size (13 Å × 34 Å), insulin easily diffuses through the large channels of NU-1000 while simultaneously requiring much longer incubation times to diffuse through the microporous channels of NU-901. Confocal laser scanning microscopy (CLSM) images revealed a dark spot in the center of the NU-1000 crystals where insulin647 was not able to diffuse and this inhibited diffusion was attributed to the presence of the microporous NU-901 phase. Contrastingly, a homogeneous distribution of insulin647 was observed throughout NU-1000-TFA (Figure 4, S4 and S5).

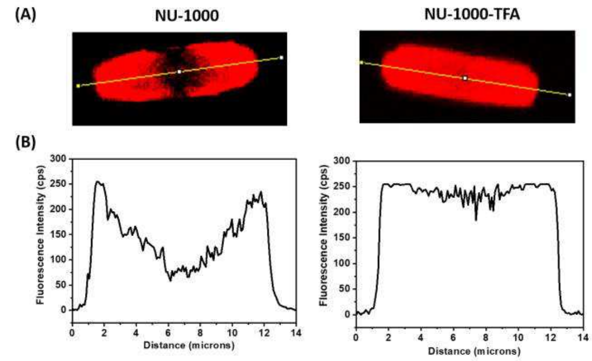

Figure 4. (A) Confocal laser scanning microscopy (CLSM) images and (B) plots of fluorescence intensity of NU-1000 and NU-1000-TFA after installation of insulin647 tagged with a fluorescent probe for 1 day at room temperature.

The limited diffusion to the center of defective NU-1000 can also be observed when the Keggin-type polyoxometalate (POM), $H_3PW_{12}O_{40}$, an anionic metal oxide cluster composed of W ions bridged by oxygen atoms with ~1 nm diameter, was employed as a probe molecule.[41] Similar to insulin647, the POM's size encumbers diffusion through the micropores of NU-901. Both NU-1000-TFA and NU-1000 were soaked in a solution of POM for 3 days and then washed thoroughly prior to energy dispersive X-ray spectroscopy (EDS) analyses. Considering the similar POM loading in both MOFs, the weaker tungsten EDS signal at the center of PW_{12}@NU-1000 crystal suggests lower loading of POM at this location (Figure 5). On the other hand, PW_{12}@NU-1000-TFA exhibited a more homogenous distribution of tungsten throughout the crystal. Limited diffusion of large probe molecules is not the only technique to support the presence of the microporous secondary phase in the center of the crystal. Installation of molybdenum on the nodes of NU-1000 by atomic layer deposition in MOFs (AIM) results in preferential deposition of molybdenum species in the center of the crystal, as

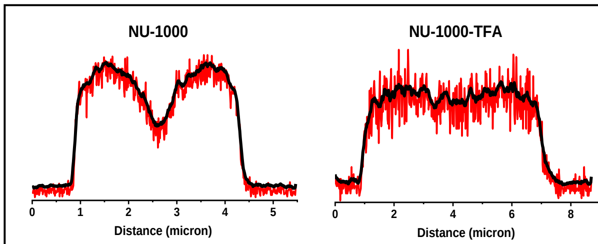

Figure 5. Tungsten EDS signal of NU-1000 and NU-1000-TFA crystals after $[PW_{12}O_{40}]^{3-}$ loading. Black lines are smoothed (adjacent averaging) for clarity.

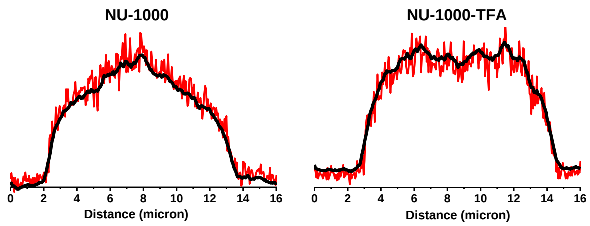

Figure 6. Molybdenum EDS signal of NU-1000 and NU-1000-TFA crystals after Mo-ALD process. Black lines are smoothed (adjacent averaging) for clarity.

evidenced from the *lamda* (Λ) shaped Mo EDS line profile (Figure 6). This is the opposite trend of the observations when larger probes were installed in NU-1000. The molybdenum hexacarbonyl ($Mo(CO)_6$) precursor is small enough to easily diffuse in the micropores of the NU-901, so preferential exclusion by the secondary-phase should not occur. Since aggregation of precursors under the ALD treatment conditions is stabilized by confinement,[46] there is preferential growth of molybdenum clusters in the denser microporous region in the center of the crystal. On the other hand, when the secondary-phase is excluded from the center of crystals, uniform distribution of molybdenum species is observed in the case of NU-1000-TFA (Figure 6).

While the use of probe molecules indirectly proves the prevention of the secondary-phase during the NU-1000-TFA growth, single crystal XRD analysis of large NU-1000-TFA crystals allows for a more quantitative evaluation of phase purity. Figure 7 shows the residual electron density maps of NU-1000 and NU-1000-TFA crystals. In NU-1000-TFA, the electron density in the mesopores resulting from the secondary-phase is approximately 6% occupied, dramatically reduced from the 25% occupancy in NU-1000, confirming the improvement in the homogeneity of the crystals.[47]

Given the potential applications of NU-1000 as an atomically ordered heterogeneous catalyst or catalyst support, we have performed a multi-gram synthesis of NU-1000-TFA; the N_2 isotherms, SEM images, and PXRD patterns confirm the purity of the scaled-up batches (Figure S1–S3).

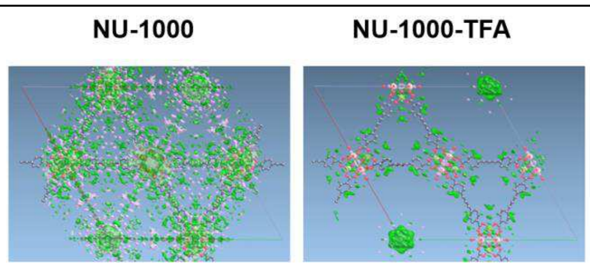

Figure 7. F_o–F_c contour maps in the *ab* plane of NU1000 and NU-1000-TFA (before using SQUEEZE program). The electron densities due to the secondary frameworks are visualized. Counters are from NU-1000 –0.96 to 0.96 eA^{-3} in steps of 0.16 eA^{-3}and NU-1000-TFA –0.64 to 0.64 eA^{-3} in steps of 0.16 eA^{-3}, respectively. The counter maps were calculated using ShelXle software.

Conclusions

In conclusion, using TFA as a co-modulator in NU-1000 synthesis controls the crystal formation and can prevent the formation of NU-901 phase at the early stage of crystallization. We have utilized large biomolecules and inorganic molecules as probes to demonstrate the elimination of secondary-phase formation in NU-1000. Single crystal X-ray diffraction analysis confirmed the significant enhancement in structural homogeneity. We have also demonstrated that the synthesis protocol developed here can be scaled-up easily to obtain multi-gram phase-pure NU-1000, which is crucial for industrial applications. Currently, we are working on understanding the role of TFA as well as exploring the underlying kinetic and thermodynamic mechanism of NU-1000 growth.

Conflicts of interest

There are no conflicts to declare.

Acknowledgements

O.K.F. gratefully acknowledges support from Defense Threat Reduction Agency (HDTRA1-18-1-0003) and Army Research Office-STTR (W911SR-17-C-0007). This work made use of the EPIC, Keck-II, and/or SPID facilities of Northwestern University's NUANCE Center, which has received support from the Soft and Hybrid Nanotechnology Experimental (SHyNE) Resource (NSF ECCS-1542205); the MRSEC program (NSF DMR-1121262) at the Materials Research Center; the International Institute for Nanotechnology (IIN); the Keck Foundation; and the State of Illinois, through the IIN.

Notes and references

1. Furukawa, H.; Cordova, K. E.; O'Keeffe, M.; Yaghi, O. M. The Chemistry and Applications of Metal-Organic Frameworks *Science* **2013,** *341*, 1230444.
2. Bai, Y.; Dou, Y.; Xie, L.-H.; Rutledge, W.; Li, J.-R.; Zhou, H.-C. Zr-Based Metal-Organic Frameworks: Design, Synthesis, Structure, and Applications *Chem. Soc. Rev.* **2016,** *45*, 2327-2367.
3. Rimoldi, M.; Howarth, A. J.; DeStefano, M. R.; Lin, L.; Goswami, S.; Li, P.; Hupp, J. T.; Farha, O. K. Catalytic Zirconium/Hafnium-Based Metal-Organic Frameworks *ACS Catal.* **2017,** *7*, 997-1014.
4. Cavka, J. H.; Jakobsen, S.; Olsbye, U.; Guillou, N.; Lamberti, C.; Bordiga, S.; Lillerud, K. P. A New Zirconium Inorganic Building Brick Forming Metal Organic Frameworks with Exceptional Stability *J. Am. Chem. Soc.* **2008,** *130*, 13850-13851.
5. Ma, J.; Tran, L. D.; Matzger, A. J. Toward Topology Prediction in Zr-Based Microporous Coordination Polymers: The Role of Linker Geometry and Flexibility *Cryst. Growth Des.* **2016,** *16*, 4148-4153.
6. Liu, T.-F.; Vermeulen, N. A.; Howarth, A. J.; Li, P.; Sarjeant, A. A.; Hupp, J. T.; Farha, O. K. Adding to the Arsenal of Zirconium-Based Metal–Organic Frameworks: The Topology as a Platform for Solvent-Assisted Metal Incorporation *Eur. J. Inorg. Chem.* **2016,** *2016*, 4349-4352.

7. Yaghi, O. M.; O'Keeffe, M.; Ockwig, N. W.; Chae, H. K.; Eddaoudi, M.; Kim, J. Reticular Synthesis and the Design of New Materials *Nature* **2003,** *423*, 705.
8. Mondloch, J. E.; Bury, W.; Fairen-Jimenez, D.; Kwon, S.; DeMarco, E. J.; Weston, M. H.; Sarjeant, A. A.; Nguyen, S. T.; Stair, P. C.; Snurr, R. Q.; Farha, O. K.; Hupp, J. T. Vapor-Phase Metalation by Atomic Layer Deposition in a Metal-Organic Framework *J. Am. Chem. Soc.* **2013,** *135*, 10294-10297.
9. Feng, D.; Gu, Z.-Y.; Li, J.-R.; Jiang, H.-L.; Wei, Z.; Zhou, H.-C. Zirconium-Metalloporphyrin Pcn-222: Mesoporous Metal–Organic Frameworks with Ultrahigh Stability as Biomimetic Catalysts *Angew. Chem. Int. Ed.* **2012,** *51*, 10307-10310.
10. Kung, C. W.; Wang, T. C.; Mondloch, J. E.; Fairen-Jimenez, D.; Gardner, D. M.; Bury, W.; Klingsporn, J. M.; Barnes, J. C.; Van Duyne, R.; Stoddart, J. F.; Wasielewski, M. R.; Farha, O. K.; Hupp, J. T. Metal-Organic Framework Thin Films Composed of Free-Standing Acicular Nanorods Exhibiting Reversible Electrochromism *Chem. Mater.* **2013,** *25*, 5012-5017.
11. Pang, J.; Yuan, S.; Qin, J.; Liu, C.; Lollar, C.; Wu, M.; Yuan, D.; Zhou, H.-C.; Hong, M. Control the Structure of Zr-Tetracarboxylate Frameworks through Steric Tuning *J. Am. Chem. Soc.* **2017,** *139*, 16939-16945.
12. Deria, P.; Gómez-Gualdrón, D. A.; Hod, I.; Snurr, R. Q.; Hupp, J. T.; Farha, O. K. Framework-Topology-Dependent Catalytic Activity of Zirconium-Based (Porphinato)Zinc(Ii) Mofs *J. Am. Chem. Soc.* **2016,** *138*, 14449-14457.
13. Wang, T. C.; Bury, W.; Gómez-Gualdrón, D. A.; Vermeulen, N. A.; Mondloch, J. E.; Deria, P.; Zhang, K.; Moghadam, P. Z.; Sarjeant, A. A.; Q.Snurr, R.; Stoddart, J. F.; T.Hupp, J.; Farha, O. K. Ultrahigh Surface Area Zirconium Mofs and Insights into the Applicability of the Bet Theory *J. Am. Chem. Soc.* **2015,** *137*, 3585-3591.
14. Liu, T.-F.; Feng, D.; Chen, Y.-P.; Zou, L.; Bosch, M.; Yuan, S.; Wei, Z.; Fordham, S.; Wang, K.; Zhou, H.-C. Topology-Guided Design and Syntheses of Highly Stable Mesoporous Porphyrinic Zirconium Metal–Organic Frameworks with High Surface Area *J. Am. Chem. Soc.* **2015,** *137*, 413-419.
15. Morris, W.; Volosskiy, B.; Demir, S.; Gándara, F.; McGrier, P. L.; Furukawa, H.; Cascio, D.; Stoddart, J. F.; Yaghi, O. M. Synthesis, Structure, and Metalation of Two New Highly Porous Zirconium Metal–Organic Frameworks *Inorg. Chem.* **2012,** *51*, 6443-6445.
16. Furukawa, H.; Gándara, F.; Zhang, Y.-B.; Jiang, J.; Queen, W. L.; Hudson, M. R.; Yaghi, O. M. Water Adsorption in Porous Metal–Organic Frameworks and Related Materials *J. Am. Chem. Soc.* **2014,** *136*, 4369-4381.
17. Bon, V.; Senkovska, I.; Baburin, I. A.; Kaskel, S. Zr- and Hf-Based Metal–Organic Frameworks: Tracking Down the Polymorphism *Cryst. Growth Des.* **2013,** *13*, 1231-1237.
18. Bennett, T. D.; Cheetham, A. K.; Fuchs, A. H.; Coudert, F.-X. Interplay between Defects, Disorder and Flexibility in Metal-Organic Frameworks *Nat. Chem.* **2016,** *9*, 11.
19. Fang, Z.; Bueken, B.; De Vos, D. E.; Fischer, R. A. Defect-Engineered Metal–Organic Frameworks *Angew. Chem. Int. Ed.* **2015,** *54*, 7234-7254.
20. Cliffe, M. J.; Wan, W.; Zou, X.; Chater, P. A.; Kleppe, A. K.; Tucker, M. G.; Wilhelm, H.; Funnell, N. P.; Coudert, F.-X.; Goodwin, A. L. Correlated Defect Nanoregions in a Metal–Organic Framework *Nat. Commun.* **2014,** *5*, 4176.
21. Feng, D. W.; Gu, Z. Y.; Chen, Y. P.; Park, J.; Wei, Z. W.; Sun, Y. J.; Bosch, M.; Yuan, S.; Zhou, H. C. A Highly Stable Porphyrinic Zirconium Metal-Organic Framework with Shp-a Topology *J. Am. Chem. Soc.* **2014,** *136*, 17714-17717.
22. Jiang, H. L.; Feng, D. W.; Wang, K. C.; Gu, Z. Y.; Wei, Z. W.; Chen, Y. P.; Zhou, H. C. An Exceptionally Stable, Porphyrinic Zr Metal-Organic Framework Exhibiting Ph-Dependent Fluorescence *J. Am. Chem. Soc.* **2013,** *135*, 13934-13938.
23. Feng, D. W.; Chung, W. C.; Wei, Z. W.; Gu, Z. Y.; Jiang, H. L.; Chen, Y. P.; Darensbourg, D. J.; Zhou, H. C. Construction of Ultrastable Porphyrin Zr Metal-Organic Frameworks through Linker Elimination *J. Am. Chem. Soc.* **2013,** *135*, 17105-17110.
24. Schaate, A.; Roy, P.; Godt, A.; Lippke, J.; Waltz, F.; Wiebcke, M.; Behrens, P. Modulated Synthesis of Zr-Based Metal–Organic Frameworks: From Nano to Single Crystals *Chem. Eur. J.* **2011,** *17*, 6643-6651.
25. Marshall, R. J.; Hobday, C. L.; Murphie, C. F.; Griffin, S. L.; Morrison, C. A.; Moggach, S. A.; Forgan, R. S. Amino Acids as Highly Efficient Modulators for Single Crystals of Zirconium and Hafnium Metal-Organic Frameworks *J. Mater. Chem. A* **2016,** *4*, 6955-6963.
26. Hu, Z.; Castano, I.; Wang, S.; Wang, Y.; Peng, Y.; Qian, Y.; Chi, C.; Wang, X.; Zhao, D. Modulator Effects on the Water-Based Synthesis of Zr/Hf Metal–Organic Frameworks: Quantitative Relationship Studies between Modulator, Synthetic Condition, and Performance *Cryst. Growth Des.* **2016,** *16*, 2295-2301.
27. Drache, F.; Bon, V.; Senkovska, I.; Getzschmann, J.; Kaskel, S. The Modulator Driven Polymorphism of Zr (Iv) Based Metal–Organic Frameworks *Phil. Trans. R. Soc. A* **2017,** *375*, 20160027.
28. Wang, T. C.; Vermeulen, N. A.; Kim, I. S.; Martinson, A. B.; Stoddart, J. F.; Hupp, J. T.; Farha, O. K. Scalable Synthesis and Post-Modification of a Mesoporous Metal-Organic Framework Called Nu-1000 *Nat. Protoc.* **2016,** *11*, 149-162.
29. Islamoglu, T.; Goswami, S.; Li, Z.; Howarth, A. J.; Farha, O. K.; Hupp, J. T. Postsynthetic Tuning of Metal-Organic Frameworks for Targeted Applications *Acc. Chem. Res.* **2017,** *50*, 805-813.
30. Mondloch, J. E.; Katz, M. J.; Isley Iii, W. C.; Ghosh, P.; Liao, P.; Bury, W.; Wagner, G. W.; Hall, M. G.; DeCoste, J. B.; Peterson, G. W.; Snurr, R. Q.; Cramer, C. J.; Hupp, J. T.; Farha, O. K. Destruction of Chemical Warfare Agents Using Metal–Organic Frameworks *Nat. Mater.* **2015,** *14*, 512-516.
31. Atilgan, A.; Islamoglu, T.; Howarth, A. J.; Hupp, J. T.; Farha, O. K. Detoxification of a Sulfur Mustard Simulant Using a Bodipy-Functionalized Zirconium-Based Metal–Organic Framework *ACS Appl. Mater. Interfaces* **2017,** *9*, 24555-24560.
32. Li, P.; Modica, J. A.; Howarth, A. J.; Vargas, E.; Moghadam, P. Z.; Snurr, R. Q.; Mrksich, M.; Hupp, J. T.; Farha, O. K. Toward Design Rules for Enzyme Immobilization in Hierarchical Mesoporous Metal-Organic Frameworks *Chem-Us* **2016,** *1*, 154-169.
33. Islamoglu, T.; Ortuño, M. A.; Proussaloglou, E.; Howarth, A. J.; Vermeulen, N. A.; Atilgan, A.; Asiri, A. M.; Cramer, C. J.; Farha, O. K. Presence Versus Proximity: The Role of Pendant Amines in the Catalytic Hydrolysis of a Nerve Agent Simulant *Angew. Chem.* **2018,** *130*, 1967-1971.
34. Drout, R. J.; Otake, K.; Howarth, A. J.; Islamoglu, T.; Zhu, L.; Xiao, C.; Wang, S.; Farha, O. K. Efficient Capture of Perrhenate and Pertechnetate by a Mesoporous Zr Metal–Organic Framework and Examination of Anion Binding Motifs *Chem. Mater.* **2018,** *30*, 1277-1284.
35. Peters, A. W.; Li, Z.; Farha, O. K.; Hupp, J. T. Atomically Precise Growth of Catalytically Active Cobalt Sulfide on Flat Surfaces and within a Metal–Organic Framework Via Atomic Layer Deposition *ACS Nano* **2015,** *9*, 8484-8490.
36. Simons, M. C.; Ortuño, M. A.; Bernales, V.; Gaggioli, C. A.; Cramer, C. J.; Bhan, A.; Gagliardi, L. C–H Bond Activation on Bimetallic Two-Atom Co-M Oxide Clusters Deposited on Zr-Based Mof Nodes: Effects of Doping at the Molecular Level *ACS Catal.* **2018,** *8*, 2864-2869.

37. Van Wyk, A.; Smith, T.; Park, J.; Deria, P. Charge-Transfer within Zr-Based Metal–Organic Framework: The Role of Polar Node *J. Am. Chem. Soc.* **2018,** *140*, 2756-2760.
38. Zhang, W.; Ma, Y.; Santos-López, I. A.; Lownsbury, J. M.; Yu, H.; Liu, W.-G.; Truhlar, D. G.; Campbell, C. T.; Vilches, O. E. Energetics of Van Der Waals Adsorption on the Metal–Organic Framework Nu-1000 with Zr6-Oxo, Hydroxo, and Aqua Nodes *J. Am. Chem. Soc.* **2018,** *140*, 328-338.
39. Desai, S. P.; Malonzo, C. D.; Webber, T.; Duan, J. X.; Thompson, A. B.; Tereniak, S. J.; DeStefano, M. R.; Buru, C. T.; Li, Z. Y.; Penn, R. L.; Farha, O. K.; Hupp, J. T.; Stein, A.; Lu, C. C. Assembly of Dicobalt and Cobalt-Aluminum Oxide Clusters on Metal-Organic Framework and Nanocast Silica Supports *Faraday Discuss.* **2017,** *201*, 299-314.
40. Li, P.; Moon, S.-Y.; Guelta, M. A.; Lin, L.; Gómez-Gualdrón, D. A.; Snurr, R. Q.; Harvey, S. P.; Hupp, J. T.; Farha, O. K. Nanosizing a Metal–Organic Framework Enzyme Carrier for Accelerating Nerve Agent Hydrolysis *ACS Nano* **2016,** *10*, 9174-9182.
41. Buru, C. T.; Li, P.; Mehdi, B. L.; Dohnalkoya, A.; Platero-Prats, A. E.; Browning, N. D.; Chapman, K. W.; Hupp, J. T.; Farha, O. K. Adsorption of a Catalytically Accessible Polyoxometalate in a Mesoporous Channel-Type Metal-Organic Framework *Chem. Mater.* **2017,** *29*, 5174-5181.
42. Liu, W.-G.; Truhlar, D. G. Computational Linker Design for Highly Crystalline Metal–Organic Framework Nu-1000 *Chem. Mater.* **2017,** *29*, 8073-8081.
43. Li, P.; Moon, S.-Y.; Guelta, M. A.; Lin, L.; Gómez-Gualdrón, D. A.; Snurr, R. Q.; Harvey, S. P.; Hupp, J. T.; Farha, O. K. Nanosizing a Metal–Organic Framework Enzyme Carrier for Accelerating Nerve Agent Hydrolysis **2016**.
44. Van de Voorde, B.; Stassen, I.; Bueken, B.; Vermoortele, F.; De Vos, D.; Ameloot, R.; Tan, J.-C.; Bennett, T. D. Improving the Mechanical Stability of Zirconium-Based Metal-Organic Frameworks by Incorporation of Acidic Modulators *J. Mater. Chem. A* **2015,** *3*, 1737-1742.
45. Noh, H.; Kung, C.-W.; Islamoglu, T.; Peters, A. W.; Liao, Y.; Li, P.; Garibay, S. J.; Zhang, X.; DeStefano, M. R.; Hupp, J. T.; Farha, O. K. Room Temperature Synthesis of an 8-Connected Zr-Based Metal–Organic Framework for Top-Down Nanoparticle Encapsulation *Chem. Mater.* **2018,** *30*, 2193-2197.
46. Gallington, L. C.; Kim, I. S.; Liu, W.-G.; Yakovenko, A. A.; Platero-Prats, A. E.; Li, Z.; Wang, T. C.; Hupp, J. T.; Farha, O. K.; Truhlar, D. G.; Martinson, A. B. F.; Chapman, K. W. Regioselective Atomic Layer Deposition in Metal–Organic Frameworks Directed by Dispersion Interactions *J. Am. Chem. Soc.* **2016,** *138*, 13513-13516.
47. Patel, H. A.; Islamoglu, T.; Liu, Z. C.; Nalluri, S. K. M.; Samanta, A.; Anamimoghadam, O.; Malliakas, C. D.; Farha, O. K.; Stoddart, J. F. Noninvasive Substitution of K^+ Sites in Cyclodextrin Metal-Organic Frameworks by Li+ Ions *J. Am. Chem. Soc.* **2017,** *139*, 11020-11023.

Table of Content Figure